

Emergent facilitation behaviors in a distinguishable-particle lattice model of glass

Ling-Han Zhang^{1,*} and Chi-Hang Lam¹

¹*Department of Applied Physics, Hong Kong Polytechnic University, Hong Kong, China*

(Dated: August 23, 2016)

We propose an interacting lattice gas model of glass characterized by particle distinguishability and self-generated disorders, implemented via site-particle-dependent random interactions. It admits exact equilibrium states directly constructible at arbitrary temperature and density. Kinetic simulations show dynamic facilitation behaviors in the glassy phase in which motions of individual voids are significant only when accelerated by other voids nearby. This provides a clear microscopic justification for the dynamic facilitation picture of structural glass.

Glassy dynamics still admits many open questions despite decades of intensive studies [1–3]. When supercooled rapidly approaching the glass transition temperature T_g , many liquids can be quenched into the glassy phase, an amorphous solid-like state without long-range order. Molecular dynamics (MD) simulations are able to capture the dramatic slowdown [4, 5], but a thorough understanding of the simulated dynamics also proves challenging. The study of simplified lattice models [6–13] is thus important. In particular, the p-spin model [7] has inspired the random first-order transition (RFOT) theory [14, 15], a leading theory of glass. A potential issue however is that the model assumes externally imposed quenched disorders rather than the expected self-generated disorders induced by the momentarily frozen system configuration. Another promising theory is dynamic facilitation [16–18] founded on kinetically constrained models (KCM) [8, 9]. An important example is a spin-facilitation model by Fredrickson and Andersen (FA) in which defects interpreted as low-density regions are allowed to evolve only when facilitated by the presence of adjacent defects [8]. A full microscopic justification of the facilitation rules still remains a challenge.

In this work, we formulate a distinguishable-particle lattice model (DPLM), which is a lattice gas model with effectively infinitely many particle-types and self-generated disorders. It can be simulated at arbitrary temperature and particle density realizing physical systems ranging from dilute gases to glasses. Interestingly, the glassy phase exhibits dynamic facilitation as an emergent property.

Model: DPLM is defined by N particles on a 2D square lattice of unit lattice constant and size L^2 with periodic boundary conditions. No more than one particle can occupy each site. Each particle is distinguishable from the others (see Fig. 1). For an occupied site i , the particle index $s_i = 1, 2, \dots, N$ denotes which particle is at site i . For convenience, we let $s_i = 0$ if the site is unoccupied, i.e. occupied by a void. The occupation number n_i is hence $n_i = 1 - \delta_{0s_i}$ where δ is the Kronecker delta.

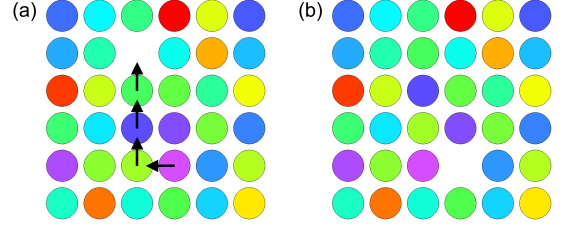


FIG. 1. (a) Schematic diagram of a region with distinguishable particles randomly colored. The arrows indicate a possible sequence of hops by four particles arranged in a line. The dynamics is equivalently described by four hops of a single void in the reversed direction. (b) The particle displacements result in distinct nearest neighboring pairings and hence different interaction energies along the *whole* path.

The whole set of s_i , rather than n_i , uniquely specifies the state of our system.

The total system energy is defined as

$$E = \sum_{\langle i,j \rangle} V_{ijs_i s_j} n_i n_j \quad (1)$$

where the sum is over all nearest neighboring (NN) sites. A key feature is the site-particle-dependent interaction energy V_{ijkl} . Its dependence on particle indices k and l means that each particle defines its own interaction strengths and this will be justified further. Effectively, each particle is a type of its own. This generalizes other multi-species models for glass [4, 12]. Before specifying V_{ijkl} , note that Eq. (1) provides a very general model at this point. For example, a constant $V_{ijkl} \equiv V$ gives a simple interacting lattice gas. As lattice gas models can be mapped to spin models with spin-exchange (Kawasaki) dynamics, it also represents a ferromagnetic or anti-ferromagnetic spin model. Alternatively, a particle-dependent $V_{ijkl} \equiv V_{kl}$ reduces it to a multi-species lattice gas such as a binary alloy [19]. More interestingly, limiting to a site-dependent $V_{ijkl} \equiv V_{ij}$, it becomes a variant of the Edwards-Anderson (EA) model for spin glass [6] with Kawasaki dynamics and a random field. Since the EA model is closely related to the p-spin model, the very definition of DPLM may appear more closely related to RFOT than dynamic facilitation.

For DPLM, each V_{ijkl} is an independent random variable following the distribution $g(V_{ijkl})$. This site-particle

* Present address: Department of Physics, Carnegie Mellon University, Pittsburgh, Pennsylvania 15213

dependence is not necessarily due to possible diverse particle properties. Instead, it is motivated by self-generated positional disorders at sub-lattice resolutions which are usually truncated in lattice models. A particle at site i in a spatially disordered system in principle admits a small random offset $\Delta\mathbf{r}_i$ from the exact lattice point. This results in a random deviation in the atomic separation \mathbf{r}_{ij} between the particles at sites i and j and hence also in the pair interaction V_{ijkl} . Rather than explicitly modeling the disorders in $\Delta\mathbf{r}_i$ or \mathbf{r}_{ij} , we directly consider the resulting random fluctuations in the interaction by simply taking a random V_{ijkl} . The dependence on both site and particle indices models the random changes expected to be induced by the hopping of any of the concerned particles or of the whole pair. Realistically, there must also be additional dependencies on further neighbors, which are all neglected for simplicity.

While V_{ijkl} is a constant for fixed indices, $V_{ij s_i s_j}$ in Eq. (1) admits a time dependence via the dynamics of s_i and s_j . Therefore, the value of $V_{ij s_i s_j}$ can persist until a relevant configurational change, and more importantly is memorized and reinstated any time the local configuration is restored after changes. This precisely characterizes self-generated disorders as opposed to quenched or simple annealed disorders. For simplicity, $g(V_{ijkl})$ is assumed to be the uniform distribution in $[-0.5, 0.5]$ which leads to a particle interaction slightly attractive on average.

A nice feature of DPLM is that equilibrium states are exactly solvable (see Appendix A). To simulate the dynamics at temperature T , each particle can hop to an unoccupied NN site at a rate [20]

$$w = w_0 \exp\left(-\frac{E_0 + \Delta E/2}{kT}\right) \quad (2)$$

where ΔE is the change in the system energy due to the hop and $k = 1$ is the Boltzmann constant. This definition satisfies detailed balance. We let $E_0 = 1.5$ so that $E_0 + \Delta E/2 \geq 0$. Also, we put $w_0 = 10^6$. Particle motions can be equivalently described as void motions (see Fig. 1). At temperature $T \rightarrow \infty$, DPLM reduces to a simple sliding block model [21].

Results: Let $\phi_v = 1 - \phi$ be the void density where $\phi = N/L^2$ is the particle density physically related to the system pressure. We perform kinetic Monte Carlo simulations of fully equilibrated systems at $L = 100$ at various T and ϕ_v (see Appendix B for simulation details). Standard dynamical measurements show that the system behaves as a simple liquid at high T and ϕ_v and a glass at low T and ϕ_v . Specifically, glassy behaviors are shown by the appearance of a plateau in the particle mean square displacement (MSD), a super-Arrhenius T dependence of the particle diffusion coefficient D , a stretched exponential form of the self-intermediate scattering function, a violation of the Stokes-Einstein relation, and typical time and T dependences of a four-point susceptibility (see Appendix C). We believe that at any finite T and ϕ_v , DPLM

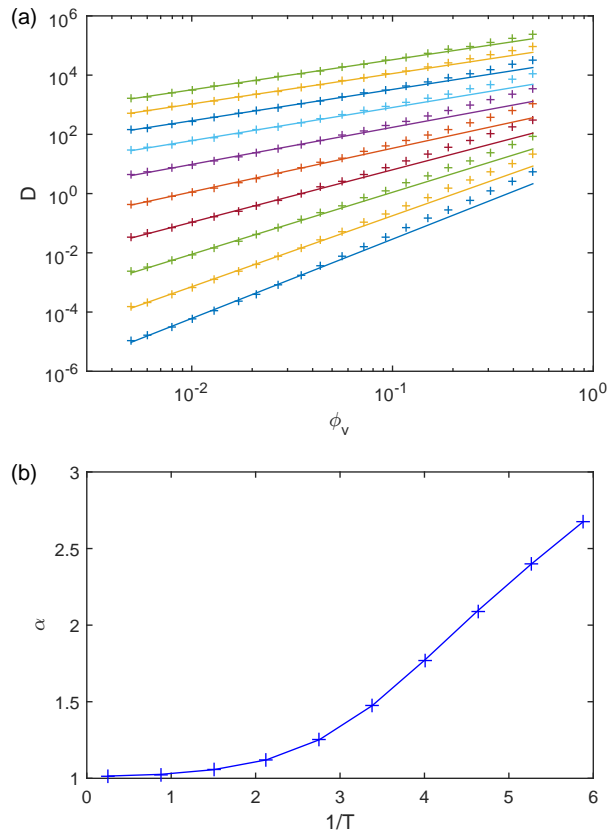


FIG. 2. (a) Particle diffusion coefficient D against void density ϕ_v in log-log scale for $T = 0.170, 0.190, 0.216, 0.250, 0.296, 0.363, 0.470, 0.666, 1.142, 4.000$, with the highest T at the top. (b) Scaling exponent α against $1/T$ obtained from linear fits to data in (a) with $\phi_v \leq 0.05$.

exhibits no ideal phase transition and is ergodic at large L .

Being an energetically non-trivial model with T and ϕ_v independently and fully tunable, it exhibits much richer physics than purely kinetic models such as KCM. We have measured D from the particle MSD at long times and results are plotted in Fig. 2(a). At each T , the linear relation in the log-log plot at small ϕ_v suggests the power-law

$$D \sim \phi_v^\alpha. \quad (3)$$

Fig. 2(b) plots the scaling exponent α as a function of T . For the liquid state at high T , we get $\alpha \simeq 1$ indicating that each void moves independently [21]. This is supported by a movie showing the void motions [22]. Fig. 3(a) also visualizes the motions using void trajectories (thin lines). They appear more compact than those of simple random walks due to the self-generated disorders. Particles with non-zero net displacements (pink and red) induced by the same void can be grouped into a cluster. Cluster sizes for different voids are relatively uniform. Voids are not trapped and travel throughout

the whole system independently at longer times. Dynamic heterogeneity revealed via these clusters is weak and short-lived.

We now explain that the low T regime exhibits dynamic facilitation [18]. Fig. 2(b) shows that α rises to 2 and beyond at low T . The nonlinear scaling dictates that voids at vanishing ϕ_v contribute to negligible dynamics. According to simple chemical kinetics, $\alpha \simeq 2$ corresponds to motion dominated by pairs of coupled voids. This quantitatively shows an emergent dynamic facilitation behavior of void motions. It is analogous to KCM and in particular the spin facilitation dynamics of the FA model [8]. We have checked that the nonlinear scaling in Eq. (3) is not due to any void aggregation and is robust upon tuning the void-void attraction by a shift of g on the energy scale.

To confirm the above facilitation interpretation of Eq. (3), we directly visualize the motion using a movie [22] and Fig. 3(b). From Fig. 3(b), the void trajectories now become even more compact with numerous dead-ends indicating back-and-forth hops due to enhanced disorders. The trajectory of each isolated void induces no or few displaced particles (pink and red) as most particles have not hopped or have returned to their original positions. In sharp contrast, a pair of voids nearby to each other induces significantly more extensive intertwining trajectories and vigorous particle displacements. Such pairs dominate the dynamics for the $\alpha \simeq 2$ regime. At longer times, isolated voids typically remain trapped locally by the disorders unless visited and untrapped by other mobile pairs. Pairs of voids may split and new pairs may emerge but these occur at a longer time scale. Dynamic heterogeneity induced by highly mobile pairs of voids among trapped isolated voids is thus strong and long-lived. Fig. 2(b) suggests that α may reach 3 and beyond at even lower T indicating dynamics dominated by triplets of voids, etc.

The confined dynamics of an isolated void at low T typically involve back-and-forth hops along low-energy paths. Note that n hops by a single void corresponds to n single-hops by n particles as shown in Fig. 1. A trapped void hence typically leads to bistable-like back-and-forth hops by a few particles. Such repetitive motions observed in MD simulations of polymers have been argued as the main cause of super-Arrhenius slow-down [23]. We have adapted the method in Ref. [23] to quantify these repetitions. After a particle has hopped, we measure the probability P_{ret} that its next hop returns itself to the original site. The probability P_2 that it next hops instead to a new site is also measured. The results for $\phi_v = 0.01$ are plotted in Fig. 4. They agree with $P_{ret} + P_2 = 1$ within 0.01% and the minor deviations are due to particles without a second hop during the observed period. At large T , we find empirically that $P_{ret} \simeq 1/2$ applicable for small ϕ_v noting that the random walks of voids induce correlated walks of particles [24]. We have checked that P_{ret} approaches towards the particle random walk value $1/4$ at large ϕ_v . As T decreases, P_{ret} in-

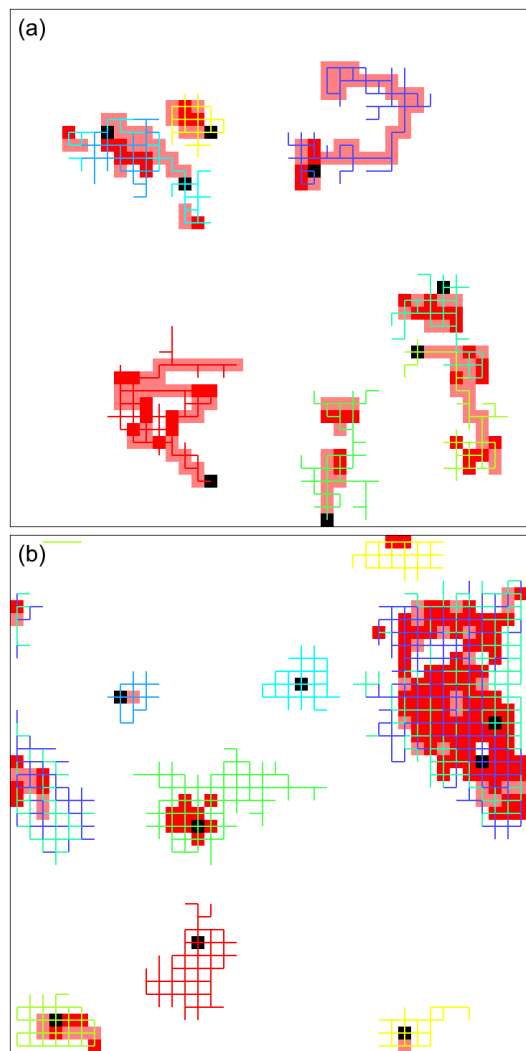


FIG. 3. (a) A snapshot from a small-scale simulation showing the final positions of voids (black squares) after a short simulation duration of $\Delta\tau = 10^{-3}$ at $T = 0.5$. Particles with net displacements 0, 1, and > 1 during the period are shaded in white, pink and red respectively. Each thin line shows the trajectory of a void and is colored randomly. (b) Similar to (a) with $T = 0.16$ and $\Delta\tau = 5 \times 10^4$. In both (a) and (b), the particle MSD during the period is about 0.5.

creases monotonically reaching 0.96 for the lowest T studied. The trend strikingly resembles those from polymer simulations [23]. This resemblance also strongly supports the physical relevance of DPLM. Such a high P_{ret} means that most hops are reversed and irrelevant to long-time dynamics. The repetition thus must contribute significantly to the slowdown. As $T \rightarrow 0$, our results support $P_{ret} \rightarrow 1$. Most hopping particles then form two-level systems (TLS) known to be relevant to glasses at very low T [25].

Conclusion: We have developed DPLM as a lattice gas model based on distinguishable particles and self-generated disorders for studying glassy dynamics. In

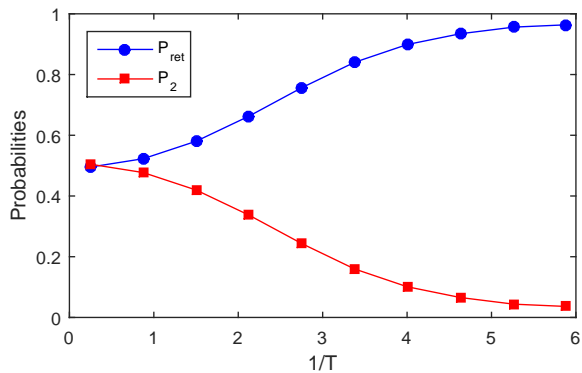


FIG. 4. Probabilities P_{ret} and P_2 for returning and non-returning second hops against $1/T$ for $\phi_v = 0.01$.

the glassy phase, the particle diffusion coefficient scales nonlinearly with the void density in the low void density limit. This implies that isolated voids are essentially trapped and the dynamics of a void is dominated by facilitation by another void nearby. Particle hopping becomes increasingly repetitive at low temperature.

DPLM is defined by a simple, generic, and physically motivated Hamiltonian. It has both non-trivial energetics and kinetics. It can be efficiently simulated and equilibrium states can be directly generated at arbitrary temperature and density. Its glassy state also does not rely on frustration on a specific lattice type. These may render DPLM a unique prototypical model for the further study of glassy dynamics and aging in disordered systems.

The definition of DPLM involves no explicit facilitation rule but facilitation behaviors are observed. It thus provides a strong microscopic support to dynamic facilitation and KCM. It will be interesting to deduce the precise coarse-grained lattice model for DPLM which is expected to be in the class of KCM. Dynamic facilitation of voids demonstrated by DPLM is analogous to the picture of facilitation via pair-interactions of string-like particle motions motivated by MD simulations of polymers [23]. In that picture, each string is initiated by a single void leading to a one-one correspondence between strings and voids. From Fig. 1, the motion of a void alters the particle pairings and hence the energy landscape experienced by other voids along its entire path. Whether another void nearby can cross the previous path is thus randomly affected. This demonstrates a form of path interaction of voids which is essentially equivalent to string interactions observed in MD [23].

As $T \rightarrow 0$, the fraction of possible states in DPLM with appreciable probabilistic weights becomes vanishingly small. Every equilibrium state is then surrounded by arbitrarily many barrier states in the phase space similar to the mosaic picture of RFOT [15]. Nevertheless, according to the void facilitation behavior observed, these equilibrium states are connected by barrierless pathways

corresponding to coupled motions of voids. The picture of activated hopping between meta-stable valleys thus is inapplicable to DPLM.

Acknowledgements: We thank helpful discussions with J.Q. You and Ho-Kei Chan. We are grateful to the support of Hong Kong GRF (Grant 15301014).

Appendix A: Exact equilibrium statistics

Despite non-trivial energetics, it is possible to derive the exact equilibrium states of DPLM because the system follows a Boltzmann distribution which factorizes over the bonds. We also assume that the system is ergodic at arbitrary temperature as is indicated by our simulations described in Appendix C. Thus, ensemble averages in the following are performed via simple annealed averaging.

For a given realization of the interactions $\{V_{ijkl}\}$, the system partition function is

$$Z = \sum_{\{s_i\}} e^{-\beta E} \quad (\text{A1})$$

where the sum is over all possible system states $\{s_i\}$ with N particles and $\beta = 1/kT$. Here, the system energy E has been defined in Eq. (1) and can be simplified to

$$E = \sum_{\langle i,j \rangle'} V_{ij s_i s_j} \quad (\text{A2})$$

where the sum is restricted to bonded NN sites i and j , i.e. with both sites occupied by particles. Eq. (A1) then becomes

$$Z = \sum_{\{s_i\}} \prod_{\langle ij \rangle'} e^{-\beta V_{ij s_i s_j}} \quad (\text{A3})$$

An ensemble averaging over $\{V_{ijkl}\}$ formally gives

$$\bar{Z} = \sum_{\{n_i\}} \sum_{\mathcal{P}\{s_i\}} \prod_{\langle ij \rangle'} \langle e^{-\beta V_{ij s_i s_j}} \rangle \quad (\text{A4})$$

where we have also rewritten the sum over all system states as a double sum over all possible site occupancies $\{n_i\}$ and the $N!$ permutations $\mathcal{P}\{s_i\}$ of the N distinguishable particles. The average free energy U of a bond between two NN particles can be written as

$$U = -\frac{1}{\beta} \ln \langle e^{-\beta V_{ij s_i s_j}} \rangle \quad (\text{A5})$$

$$= -\frac{1}{\beta} \ln \int_{-\infty}^{\infty} e^{-\beta V} g(V) dV \quad (\text{A6})$$

Here, U is independent of s_i as all particles have identical statistical properties. Therefore, all permutations of s_i contribute equally to \bar{Z} and we have

$$\bar{Z} = N! \sum_{\{n_i\}} \prod_{\langle ij \rangle'} e^{-\beta U} \quad (\text{A7})$$

Omitting the physically irrelevant constant factor and simplifying, we get

$$\bar{Z} = \sum_{\{n_i\}} e^{-\beta N_b U} \quad (\text{A8})$$

where N_b is the number of pairs of bonded particles for the given occupation configuration $\{n_i\}$. Now, \bar{Z} is formally identical to the partition function of a simple identical-particle lattice gas with a NN particle interaction energy U . The two systems hence have exactly the same equilibrium statistics despite the very different dynamics.

In DPLM, each particle interaction is in principle sampled from the probability density g . The probability density of a specific realization of $\{V_{ijkl}\}$ is simply

$$P(\{V_{ijkl}\}) = \prod_{\langle i,j \rangle, k, l} g(V_{ijkl}) \quad (\text{A9})$$

where the product is over all NN sites i, j and particles $k, l = 1, 2, \dots, N$. Requiring further that the system is at a specific equilibrium state $\{s_i\}$, the probability density becomes

$$P_{eq}(\{V_{ijkl}\}) \propto e^{-\beta E} \prod_{\langle i,j \rangle, k, l} g(V_{ijkl}) \quad (\text{A10})$$

Applying Eq. (A2), we get

$$P_{eq}(\{V_{ijkl}\}) \propto \prod_{\langle i,j \rangle'} e^{-\beta V_{ij s_i s_j}} g(V_{ij s_i s_j}) \prod_C g(V_{ijkl}) \quad (\text{A11})$$

Here, factors in the first product implies that the interaction $V_{ij s_i s_j}$ of every bond existing in the state $\{s_i\}$ follows the Boltzmann distribution

$$p_{eq}(V_{ij s_i s_j}) \propto e^{-\beta V_{ij s_i s_j}} g(V_{ij s_i s_j}) \quad (\text{A12})$$

with the role of g analogous to a density of state function. The second product is over the complementary set C containing all non-bonded V_{ijkl} which do not explicitly appear in the state $\{s_i\}$. Eq. (A11) implies that every non-bonded V_{ijkl} simply follows $g(V_{ijkl})$.

Appendix B: Simulation details

Using accelerated algorithms to be explained below, each of our main simulations performed at $L = 100$ takes up to about 20 hours to run on an Intel Xeon processor core. Data for each set of values of T and ϕ_v are typically averaged over 5 similar independent runs. Additional shorter runs recording particle positions at a higher time-resolution are also need to obtain correlation data at short time.

We first describe an elementary approach for equilibrium simulation of DPLM at temperature T . Before simulation starts, each distinct bond energy V_{ijkl} is independently sampled from the probability distribution g after

taking into account the symmetry $V_{ijkl} = V_{jilk}$. A random initial system configuration is constructed by distributing the N particles randomly onto the L^2 lattice points and this initializes s_i . Kinetic Monte Carlo simulation can then be performed. At each time step Δt , the followings are performed:

- Randomly choose a site i .
- Randomly choose a site j which is a NN of i .
- If $n_i = 1$ and $n_j = 0$ is false, reject this step.
- Accept particle hop from i to j with probability $4L^2 w \Delta t$ where w is calculated using Eq. (2)

Here, Δt must be small and satisfies $4L^2 w \Delta t \leq 1$ for all possible configurations.

Thermalization Monte Carlo steps will first be conducted until equilibrium is reached as indicated for example by the stabilization of the total energy E from Eq. (1). Then, main simulation steps can be performed for statistical measurements.

Rejection-free method: The simple kinetic Monte Carlo algorithm above is inefficient due to too many rejected move attempts. A rejection-free method [26] is much more efficient. Let $N_v = L^2 - N$ be the number of voids. We optimize our algorithm for ϕ_v close to 0 which is most demanding due to the slow dynamics. The number of possible hops is $4N_v$ in general. The associated hopping rates w are calculated and stored at the lowest level of a complete binary tree. Each parent node then stores the sum of the two immediate children. Note that an exchange of two voids is unphysical and is assigned a rate 0.

For each time step Δt , one of the $4N_v$ possible hops is randomly selected with a relative probability w . The selection of the hop is done efficiently by randomly descending the binary tree using the node values as the relative probabilistic weight. The hop is then executed. A few hopping rates associated with the hopping particle and its neighbors are recalculated since the local configuration has changed. The binary tree is then also updated accordingly. It is easy to see that Δt is time dependent and follows $\Delta t = 1/w_{root}$ [27]. Here, w_{root} is the value at the root which also equals the sum of all the $4N_v$ rates.

Interaction energies tabulation: A nontrivial point in the programming for DPLM is that the total number of V_{ijkl} is of order $N^2 L^2 \sim L^6$. This requires too much memory storage for large L . For medium values of L , V_{ijkl} can be sampled only when needed and stored using a hash data structure. In our main simulations with a large $L = 100$, it is necessary to adopt a permuted energy approximation to be explained below. We have checked in medium scale simulations that it gives results statistically identical to those using the hash-table method.

In our permuted energy approximation, we put

$$V_{ijkl} = v(Q_i(k), Q_j(l)) \quad (\text{B1})$$

Here, each Q_i for site i is an independent random permutation function mapping the set $1, 2, \dots, N$ to itself. The function v thus involves only order $N^2 \sim L^4$ tabulated random numbers sampled from g which are independent from each other except when the symmetry $v(k, l) = v(l, k)$ applies. Before simulation starts, the functions v and Q_i are randomly sampled and stored. The memory requirement significantly decreases from order L^6 to order L^4 .

Efficient equilibration: System equilibration using thermalization Monte Carlo steps from arbitrary initial conditions can take very long runtime and is even impractical at low T . This is a major difficulty for all MD simulations and many lattice models of glass. Being able to directly construct equilibrium states is thus a highly desirable property. This is possible for KCM with trivial energetics, non-spatial models [28, 29] and some frustrated spin models defined on triangular or related lattices [30]. DPLM is to our knowledge the only finite-dimensional and energetically non-trivial model defined on a general lattice with this capability.

We now explain how to sample a random state of DPLM from the equilibrium ensemble. First, to get s_i , we can perform a simple lattice gas simulation with a constant NN particle interaction energy U given in Eq. (A5). We do that using the same computer code for DPLM with V_{ijkl} reduced to a constant U . Equilibrating the simple lattice gas by a thermalization simulation run from an arbitrary initial state is very efficient because of the absence of glassification at arbitrary T . According to Eq. (A8), the thermalized positions give s_i appropriate for DPLM.

Second, to find V_{ijkl} , we note that Eq. (A11) implies that interactions are classified into bonded and non-bonded ones depending on whether they appear in the system state s_i . We randomly generate all non-bonded V_{ijkl} from the distribution g while bonded interactions $V_{ijs_i s_j}$ are sampled from the Boltzmann distribution in Eq. (A12). As we also adopt the permuted energy approximation in Eq. (B1), some permutations of bonded interactions will follow Eq. (A12) while they should follow g . However, only of the order $1/L^2$ of all the interactions are affected and the impacts are negligible for large L . We have verified numerically that with this equilibration approach, no measurement indicates any aging effect as expected.

Software reliability: Correct software implementation is highly nontrivial because minor programming mistakes may affect the particle dynamics only occasionally and can be very difficult to spot. One helpful consistency check is to measure the probability distribution of the interaction energy $V_{ijs_i s_j}$ at equilibrium and compare with the exact distribution in Eq. (A12). We have also conducted more general Boltzmann distribution tests [27] by performing long simulations using a small lattice with all but several particles frozen. Then, only a few thousand different configurations will be realized. We measure the

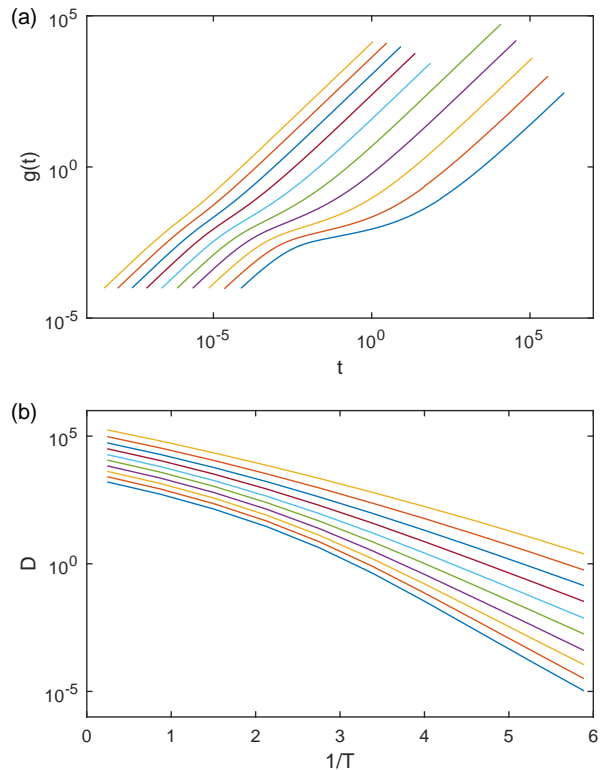


FIG. 5. (a) Mean square displacement (MSD) $g(t)$ against t in log-log scale for the same values of T used in Fig. 2(a) and $\phi_v = 0.01$ with the highest T at the top. (b) Arrhenius plot of D , for void concentrations $\phi_v = 0.005, 0.008, 0.013, 0.021, 0.035, 0.056, 0.092, 0.149, 0.242, 0.392$, with the highest ϕ_v at the top. The same data is used in Fig. 2(b).

total occurrence durations and the system energies of all these configurations and make sure that the results agree with the Boltzmann distribution within the expected statistical errors. With these tests, we believe that our software implementation is highly reliable.

Appendix C: Glassy dynamics characterizations

Diffusion coefficient: We calculate the particle mean square displacement (MSD) defined as

$$g(t) = \langle |\mathbf{r}_l(t) - \mathbf{r}_l(0)|^2 \rangle \quad (\text{C1})$$

where $\mathbf{r}_l(t)$ denotes the lattice position vector of particle l at time t . Fig. 5(a) shows $g(t)$ in a log-log plot for different T and $\phi_v = 0.01$. For $t \rightarrow \infty$, the slopes of the lines are consistent with unity, indicating diffusive behaviors over long observation time. Sub-diffusive plateaus appearing at intermediate t at low T indicate cage effects. Note that being a lattice model without vibrational modes at the sublattice level, the plateaus are much less pronounced as have been found for other lattice models [10].

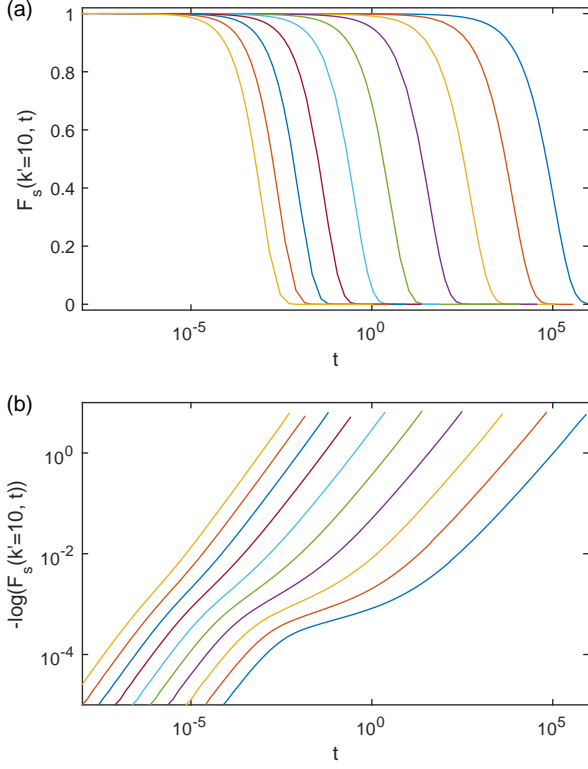


FIG. 6. (a) Decays of self-intermediate scattering function $F_s(k, t)$ in linear-log scale, for the same values of T used in Fig. 2(a), with T decreasing from left to right. Wavenumber $k = (2\pi/L)k' = \pi/5$ and $\phi_v = 0.01$ are used here. (b) Same data as in (a) in log-log-versus-log scale. Data corresponding to $F_s(k, t) < 10^{-3}$ are noisy and are omitted. The slope of the linear region at large t with $10^{-3} \leq F_s(k, t) \leq 0.9$ gives the stretching exponent β .

From similar MSD for various T and ϕ_v , we measure the particle diffusion coefficient

$$D = \frac{1}{2d} \lim_{t \rightarrow \infty} \frac{g(t)}{t} \quad (\text{C2})$$

by fitting to data points where $g(t) > 1$ and the slope is higher than 0.96. Fig. 5(b) shows D in an Arrhenius plot for various ϕ_v . It exhibits super-Arrhenius behavior which becomes more pronounced at small ϕ_v and low T . This shows that DPLM is a fragile glass.

Self-intermediate scattering function: We have measured the self-intermediate scattering function defined as

$$F_s(k, t) = \left\langle e^{i\mathbf{k} \cdot (\mathbf{r}_i(t) - \mathbf{r}_i(0))} \right\rangle \quad (\text{C3})$$

and the result is shown in Fig. 6(a) for $\phi_v = 0.01$ and $k = (2\pi/L)k'$ with $k' = 10$. A one-step drop of $F_s(k, t)$ versus t instead of a two-step decay is again typical for lattice models [10, 12, 31]. In glassy systems, the terminal decay of the scattering function is usually well approximated by

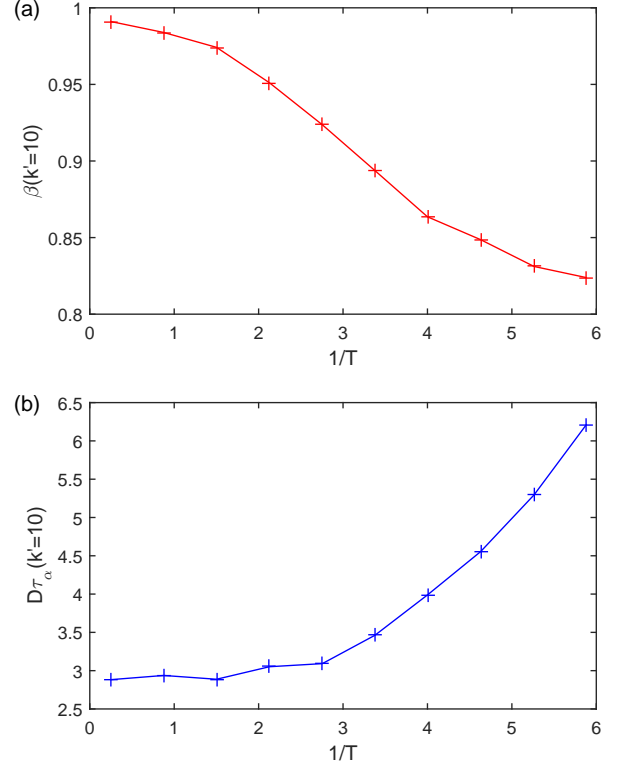


FIG. 7. (a) Stretching exponent β plotted against $1/T$ for $\phi_v = 0.01$. (b) Violation of the Stokes-Einstein relation, $D\tau_\alpha = \text{constant}$ where τ_α is a relaxation time.

the Kohlrausch-Williams-Watts (KWW) stretched exponential function of the form $A \exp(-(t/\tau)^\beta)$, where τ is a relaxation time and β ($0 < \beta < 1$) is the stretching exponent. Our results fit well to the KWW form for large t . This is also demonstrated by the log-log plot of $-\log(F_s(k, t))$ against t in Fig. 6(b) which shows a linear region at large t expected from the KWW form with $A \simeq 1$. The stretching exponent obtained from the slope of the linear region is plotted in Fig. 7(a). As T decreases, β drops from 1 to around 0.82, indicating glassy dynamics at low T .

From Fig. 6(a), we also extract a relaxation time τ_α which is the time at which $F_s(k, t) = 1/e$. Fig. 7(b) plots $D\tau_\alpha$ against $1/T$. The value clearly increases with decreasing time and demonstrate a violation of the Stokes-Einstein relation expected for glasses.

Four-point correlation function: Close to the glass transition, one region in a glassy fluid can relax much faster than another one. This spatially inhomogeneous dynamical behavior is known as dynamic heterogeneity. To quantitatively study the heterogeneity in the persistence of the particle configuration, one can define an overlap function as

$$c_l(t, 0) = e^{i\mathbf{k} \cdot (\mathbf{r}_l(t) - \mathbf{r}_l(0))}. \quad (\text{C4})$$

It measures how much particle l moves during times 0 and

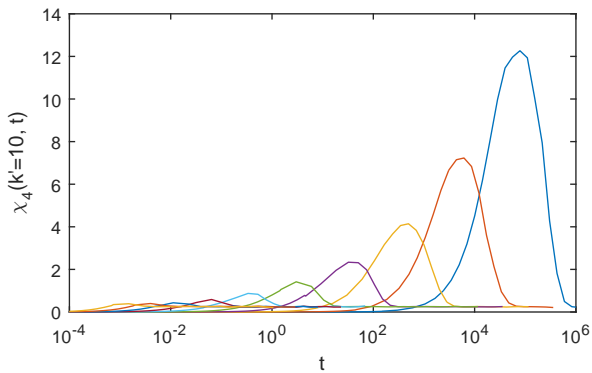


FIG. 8. $\chi_4(t)$ for $\phi_v = 0.01$ and the same values of T used in Fig. 2(a). T decreases from left to right.

t at a length scale $2\pi/k$. Note that the average overlap equals the self-intermediate scattering function $F_s(\mathbf{k}, t)$. Each particle contributes to an overlap field defined by

$$c(\mathbf{r}; t, 0) = \sum_l c_l(t, 0) \delta(\mathbf{r} - \mathbf{r}_l(0)) \quad (\text{C5})$$

Consider its spatial correlation

$$G_4(\mathbf{r}, t) = \langle c(\mathbf{r}; t, 0)c(\mathbf{0}; t, 0) \rangle - \langle c(\mathbf{0}; t, 0) \rangle^2 \quad (\text{C6})$$

where the average is over the spatial origin $\mathbf{0}$ and the starting time 0. G_4 measures the correlation of the fluctuations in the overlap function between two points that are separated by \mathbf{r} .

In the Fourier space, we get

$$S_4(\mathbf{q}, t) = \int e^{i\mathbf{q}\cdot\mathbf{r}} G_4(\mathbf{r}, t) d\mathbf{r} \quad (\text{C7})$$

$$= N \left\langle \left| \frac{1}{N} \sum_l e^{i\mathbf{q}\cdot\mathbf{r}_l(0)} (c_l(t, 0) - F_s(\mathbf{k}, t)) \right|^2 \right\rangle \quad (\text{C8})$$

One can define the susceptibility as $\chi_4(t) = \lim_{q \rightarrow 0} S_4(\mathbf{q}, t)$, which is simply the variance of the overlap function. $\chi_4(t)$ can be interpreted as the typical size of correlated clusters in structural relaxation, thus an efficient measure of the degree of dynamic heterogeneity.

Fig. 8 shows $\chi_4(t)$ from DPLM simulations. As is typical for structural glasses, for each temperature, $\chi_4(t)$ has a peak, which shifts to larger times, and has a larger value when T decreases. This reveals an increasing length scale of dynamic heterogeneity when the system cools down.

-
- [1] G. Biroli and J. P. Garrahan, *J. Chem. Phys.* **138**, 12A301 (2013).
- [2] F. H. Stillinger and P. G. Debenedetti, *Annu. Rev. Condens. Matter Phys.* **4**, 263 (2013).
- [3] L. Berthier and G. Biroli, *Rev. Mod. Phys.* **83**, 587 (2011).
- [4] W. Kob and H. C. Andersen, *Phys. Rev. E* **51**, 4626 (1995).
- [5] K. Kremer and G. S. Grest, *J. Chem. Phys.* **92**, 5057 (1990).
- [6] S. F. Edwards and P. W. Anderson, *Journal of Physics F: Metal Physics* **5**, 965 (1975).
- [7] T. R. Kirkpatrick and D. Thirumalai, *Phys. Rev. B* **36**, 5388 (1987).
- [8] G. H. Fredrickson and H. C. Andersen, *Phys. Rev. Lett.* **53**, 1244 (1984).
- [9] R. G. Palmer, D. L. Stein, E. Abrahams, and P. W. Anderson, *Phys. Rev. Lett.* **53**, 958 (1984).
- [10] W. Kob and H. C. Andersen, *Phys. Rev. E* **48**, 4364 (1993).
- [11] G. Biroli and M. Mézard, *Phys. Rev. Lett.* **88**, 025501 (2001).
- [12] R. K. Darst, D. R. Reichman, and G. Biroli, *J. Chem. Phys.* **132**, 044510 (2010).
- [13] N. B. Tito, J. E. Lipson, and S. T. Milner, *Soft Matter* **9**, 3173 (2013).
- [14] T. R. Kirkpatrick, D. Thirumalai, and P. G. Wolynes, *Phys. Rev. A* **40**, 1045 (1989).
- [15] T. R. Kirkpatrick and D. Thirumalai, *Rev. Mod. Phys.* **87**, 183 (2015).
- [16] F. Ritort and P. Sollich, *Adv. Phys.* **52**, 219 (2003).
- [17] J. P. Garrahan, P. Sollich, and C. Toninelli, *Dynamical heterogeneities in glasses, colloids and granular media*, edited by L. Berthier, G. Biroli, J.-P. Bouchaud, L. Cipelletti, and W. van Saarloosand (Oxford University Press) (2011).
- [18] D. Chandler and J. P. Garrahan, *Annu. Rev. Phys. Chem.* **61**, 191 (2010).
- [19] K. Binder, *Zeitschrift für Physik* **267**, 313 (1974).
- [20] K. A. Fichtorn and M. Scheffler, *Phys. Rev. Lett.* **84**, 5371 (2000).
- [21] Ajay and R. G. Palmer, *J. Phys. A* **23**, 2139 (1990).
- [22] Void dynamics movies available at <http://apricot.ap.polyu.edu.hk/dplm>.
- [23] C.-H. Lam and O. K. C. Tsui, arXiv:1508.03153 (2015).
- [24] M. Brummelhuis and H. Hilhorst, *Journal of statistical physics* **53**, 249 (1988).
- [25] W. Phillips, *Rep. Prog. Phys.* **50**, 1657 (1987).
- [26] A. Bortz, M. Kalos, and J. Lebowitz, *Journal of Computational Physics* **17**, 10 (1975).
- [27] C.-H. Lam, M. Lung, and L. M. Sander, *Journal of Scientific Computing* **37**, 73 (2008).
- [28] B. Derrida, *Phys. Rev. Lett.* **45**, 79 (1980).
- [29] F. Ritort, *Phys. Rev. Lett.* **75**, 1190 (1995).
- [30] M. Newman and C. Moore, *Phys. Rev. E* **60**, 5068 (1999).
- [31] P. Harrowell, *Phys. Rev. E* **48**, 4359 (1993).